A Novel Series of Vanadium-Sulfite Polyoxometalates: Synthesis, Structural, and Physical Studies

Haralampos N. Miras,[a] Raphael G. Raptis,[b] Nikolia Lalioti,[c] Michael P. Sigalas,*[d] Peter Baran,*[b] and Themistoklis A. Kabanos*[a]

Dedicated to Professor Francis Sécheresse on the occasion of his 60th birthday

Abstract: Reaction of NH_4VO_3 with sulfur dioxide affords the hexanuclear cluster $(NH_4)_2(Et_4N)[(V^{IV}O)_6(\mu_4\text{-}O)_2(\mu_3\text{-}OH)_2(\mu_3\text{-}SO_3)_4(H_2O)_2]Cl\cdot H_2O$ (**1**), and the decapentanuclear host–guest compound $(Et_4N)_5\{Cl\subset[(VO)_{15}(\mu_3\text{-}O)_{18}(\mu\text{-}O)_3]\}\cdot 3H_2O$ (**2**). Sequential addition of magnesium oxide to an acidic aqueous solution of NH_4VO_3 ($pH\approx 0$) followed by $(NH_4)_2SO_3$ resulted in the formation of either the non-oxo polymeric vanadium(IV) compound *trans*-$(NH_4)_2[V^{IV}(OH)_2(\mu\text{-}SO_3)_2]$ (**3**) or the polymeric oxovanadium(IV) sulfite $(NH_4)[V^{IV}O(SO_3)_{1.5}(H_2O)]\cdot 2.5H_2O$ (**4**) at pH values of 6 and 4, respectively. The decameric vanadium(V) compound $\{Na_4(\mu\text{-}H_2O)_8(H_2O)_6][Mg(H_2O)_6][V^V_{10}(O)_8(\mu_6\text{-}O)_2(\mu_3\text{-}O)_{14}]\cdot 3H_2O$ (**5**) was synthesised by treating an acidic aqueous solution of NH_4VO_3 with MgO and addition of NaOH to $pH\approx 6$. All the compounds were characterised by single-crystal X-ray structure analysis. The crystal structure of compound **1** revealed an unprecedented structural motif of a cubane unit $[M_4(\mu_4\text{-}O)_2(\mu_3\text{-}OH)_2]$ connected to two other metal atoms. Compound **3** comprises a rare example of a non-oxo vanadium(IV) species isolated from aqueous solution and in the presence of the reducing agent SO_3^{2-}, while compound **4** represents a rare example of an open-framework species isolated at room temperature (20 °C). In addition to the synthesis and crystallographic studies, we report the IR and magnetic properties (for **1**, **2** and **3**) of these vanadium clusters as well as theoretical studies on compound **3**.

Keywords: density functional calculations · polyoxometalates · structure elucidation · sulfites · vanadium

Introduction

Research involving polyoxometalates is driven not only by their remarkable structural and electronic properties,[1–5] but also because of their significance in quite diverse disciplines ranging from photochromism,[6] electrochromism,[7] and magnetism[1,2c] to catalysis[1] and medicine.[8] Although the polyoxometalate derivatives incorporating inorganic ligands[9–13] and in particular the tetrahedral phosphate[14] ion, have been intensively investigated in the last two decades, the polyoxometalates containing the pyramidal sulfite ion are comparatively unexplored.[15,16] This is unexpected for three main reasons: 1) metal sulfite chemistry is very attractive in view of its potential for restricting the serious environmental problem of acid rain,[17] 2) the sulfite anion has a C_{3v} symmetry and contains a non-bonding, but stereochemically active pair of electrons and its non-centrosymmetric compounds, may potentially display non-linear optical properties[18] which are observed in non-centrosymmetric metal selenites[19] and metal iodates[20] and 3) V_2O_5 is used as an in-

[a] H. N. Miras, Prof. T. A. Kabanos
Department of Chemistry, Section of Inorganic and Analytical Chemistry
University of Ioannina
45110 Ioannina (Greece)
Fax: (+30) 2651-0-44831
E-mail: tkampano@cc.uoi.gr

[b] Dr. R. G. Raptis, Dr. P. Baran
Department of Chemistry, University of Puerto Rico
Rio Piedras, P.O. San Juan, PR 00931–3346 (Puerto Rico)

[c] Dr. N. Lalioti
Department of Materials Science, University of Patras
26504 Patras (Greece)

[d] Dr. M. P. Sigalas
Department of Chemistry, Laboratory of Applied Quantum Chemistry
Aristotle University of Thessaloniki
54124 Thessaloniki (Greece)

 DOI: 10.1002/chem.200400203

dustrial catalyst in the production of sulfuric acid by oxidation of SO_2 to SO_3 at 400–600 °C.[21] Crude oil may contain up to 4% vanadium mainly in the form of $V^{IV}O^{2+}$ porphyrins,[22] which are transformed to V_2O_5 on burning. The existence of V_2O_5 in the atmosphere may cause health hazards and the oxidation of SO_2 to SO_3 (acid rain). On the other hand, it is essential to use more efficient catalysts for the industrial oxidation of SO_2 to SO_3 that will allow us to reduce the temperature for this process. Thus, it is of vital importance to study the interaction of vanadium with the sulfite anion.

We present herein the first systematic study of metal–sulfite interactions. More specifically, the synthesis and structural characterisation of the vanadium(IV) sulfite compounds **1**, **3**, and **4** are reported (see Scheme 1). In addition, IR, UV/Vis, magnetic properties and density functional calculations (for compound **3**) are reported as well. Furthermore, the synthesis, structural and physicochemical characterisation of the compounds **2** and **5** are described (see Scheme 1). A preliminary report of this research has been communicated previously.[16b]

Results and Discussion

Syntheses: The synthesis of the oxovanadium(IV)-sulfite compounds **1**, **1′**, **1″**, **3** and **4** as well as of the spherical mixed-valence host–guest cluster **2** and of the magnesium–vanadium(V) compound **5** is summarised in Scheme 1. The hexanuclear vanadium cluster **1**, was prepared by dissolving NH_4VO_3 in acidic aqueous solution (pH 0), because NH_4VO_3 is only very slightly soluble in water, then adding a concentrated aqueous ammonia to the vanadium(V) solution to pH 8. Sulfur dioxide was then bubbled through the mixture in the presence of Et_4NCl until pH was 4.5. Dark green crystals of $(Et_4N)_5[Cl\subset(V^{IV}O)_7(V^{V}O)_8(\mu_3\text{-}O)_{18}(\mu\text{-}O)_3]\cdot H_2O$ (**2**) were also formed along with the crystals of **1**, which were manually separated. The synthesis and crystallographic characterisation of $(Me_4N)_6[Cl\subset(V^{IV}O)_8(V^{V}O)_7(\mu_3\text{-}O)_{18}(\mu\text{-}O)_3]$ (**2′**),[23] obtained from the hydrolysis VS_4^{3-}, and of $(Bu_4N)_4[Cl\subset(V^{IV}O)_6(V^{V}O)_9(\mu_3\text{-}O)_{18}(\mu\text{-}O)_3]$ (**2″**),[24] obtained from $n$$Bu_4NVO_3$ in CH_3CN, have been reported in the literature. It is obvious that the anions of the clusters **2**, **2′** and **2″** differ only in their V^{IV}/V^{V} content.

In an effort to study the effect of two outer oxovanadium(IV) cations on the magnetic properties of **1**, we tried to substitute them with two non-magnetically interacting divalent metal ions (i.e., Zn^{2+}, Ca^{2+}, Mg^{2+}, etc.). Thus, sequential addition of excess MgO to an acidic aqueous solution of NH_4VO_3 (pH 0) and then of $(NH_4)_2SO_3$ resulted in the formation of either the polymeric non-oxo vanadium(IV) compound *trans*-$(NH_4)_2[V^{IV}(OH)_2(\mu\text{-}SO_3)_2]$ (**3**) or the polymeric oxovanadium(IV)-sulfite compound $(NH_4)[V^{IV}O(SO_3)_{1.5}\text{-}H_2O]\cdot 2.5H_2O$ (**4**) at pH 6 and pH 4, respectively. When the reaction was performed in the absence of MgO, the hexanuclear compound[16b] $(NH_4)_2[(V^{IV}O)_6(\mu_4\text{-}O)_2(\mu_3\text{-}OH)_2(\mu_3\text{-}SO_3)_4(H_2O)_2]$ (**1′**) was isolated instead. Compound **1′** was also synthesised by reacting $[V^{IV}OCl_2(thf)_2]$, in acidic aqueous solution, with $(NH_4)_2SO_3$.[16b] The tetrabutylammonium analogue of **1′**, $(n$$Bu_4N)_2[(V^{IV}O)_6(\mu_4\text{-}O)_2(\mu_3\text{-}OH)_2(\mu_3\text{-}SO_3)_4(H_2O)_2]$ (**1″**), was prepared by reacting $[V^{IV}OCl_2(thf)_2]$, in acidic aqueous solution, with Na_2SO_3 and $n$$Bu_4NBr$.[16b]

To answer the question: "what is the role of MgO?", the compound $\{Na_4(\mu\text{-}H_2O)_8(H_2O)_6\}[Mg(H_2O)_6][V^{V}{}_{10}(O)_8(\mu_6\text{-}O)_2(\mu_3\text{-}O)_4(\mu\text{-}O)_{14}]\cdot 3H_2O$ (**5**) was synthesised by treating an acidic aqueous solution of NH_4VO_3 (pH 0) with MgO and NaOH (to pH 6). Based on the isolation and characterisation of compound **5**, it is rather difficult to comment on the role of MgO in the isolation of compounds **3** and **4** instead of the hexanuclear vanadium(IV) clusters **1** and **1′**.

Abstract in Greek:

Η αντίδραση του NH_4VO_3 με διοξείδιο του θείου δίνει την εξαπυρηνική ένωση $(NH_4)_2(Et_4N)[(V^{IV}O)_6(\mu_4\text{-}O)_2(\mu_3\text{-}OH)_2(\mu_3\text{-}SO_3)_4(H_2O)_2]Cl\cdot H_2O$ **1** καί τη δεκαπενταμερή ένωση $(Et_4N)_5\{Cl\subset[(VO)_{15}(\mu_3\text{-}O)_{18}(\mu\text{-}O)_3]\}\cdot 3H_2O$ **2**. Διαδοχική προσθήκη οξειδίου του μαγνησίου σε ένα όξινο υδατικό διάλυμα του NH_4VO_3 (pH ≈ 0) και στη συνέχεια $[NH_4]_2SO_3$ κατέληξε στο σχηματισμό είτε της πολυμερούς ένωσης του «γυμνού» βαναδίου(IV) *trans*-$(NH_4)_2[V^{IV}(OH)_2(\mu\text{-}SO_3)_2]$ **3** ή της πολυμερούς ένωσης του οξοβαναδίου(IV)-θειωδών $(NH_4)[V^{IV}O(SO_3)_{1.5}(H_2O)]\cdot 2.5H_2O$ **4** σε τιμές pH 6 *και* 4 αντίστοιχα. Η δεκαμερής ένωση του βαναδίου(V) $\{Na_4(\mu\text{-}H_2O)_8(H_2O)_6\}[Mg(H_2O)_6][V^{V}{}_{10}(O)_8(\mu_6\text{-}O)_2(\mu_3\text{-}O)_{14}]\cdot 3H_2O$ **5** συντέθηκε με αντίδραση του NH_4VO_3 σε όξινο υδατικό διάλυμα με MgO και προσθήκη NaOH μέχρι pH≈6.

Όλες οι ενώσεις χαρακτηρίστηκαν με κρυσταλλογραφία ακτίνων X. Η κρυσταλλοδομή της ένωσης **1** αποκάλυψε ένα καινούργιο δομικό μοτίβο στο οποίο ο κύβος, $[M_4(\mu_4\text{-}O)_2(\mu_3\text{-}OH)_2]$, είναι ενωμένος με δύο άλλα μέταλλα. Η ένωση **3** αποτελεί ένα σπάνιο παράδειγμα ένωσης «γυμνού» βαναδίου(IV) που απομονώθηκε από υδατικό διάλυμα στο οποίο υπήρχε το αναγωγικό θειώδες ανιόν, ενώ η ένωση **4** αποτελεί ένα σπάνιο παράδειγμα ένωσης ανοικτού πλαισίου που απομονώθηκε στη θερμοκρασία περιβάλλοντος (20 °C). Επιπλέον της σύνθεσης και της κρυσταλλογραφικής μελέτης, οι μαγνητικές ιδιότητες (για **1**, **2** *και* **3**), η φασματοσκοπία υπερύθρου, καθώς επίσης και η θεωρητική μελέτη της ένωσης **3** αναφέρονται σε αυτή τη μελέτη.

X-ray crystallography: Selected interatomic distances and bond angles relevant to the vanadium coordination sphere for compounds **1**, **2** and **3** are listed in Table 1, Table 2 and Table 3, respectively.

X-ray structural analysis of **1** revealed the presence of the discrete cluster $[V^{IV}O)_6(\mu_4\text{-}O)_2(\mu_3\text{-}OH)_2(\mu_3\text{-}SO_3)_4(H_2O)_2]^{2-}$ (Figure 1A) as well as one Et_4N^+, two ammonium and one chloride counterions. The core of the hexanuclear cluster consists of a distorted cubane unit, $[V_4{}^{IV}(\mu_4\text{-}O)_2(\mu_3\text{-}OH)_2]$. The two outer vanadium(IV) atoms V3/V3A are connected to the cubane core through the two $\mu_4\text{-}O^{2-}$ and the four μ_3-(*O*,*O*,*O*) sulfite bridges, and their geometries lie between square-pyramidal and trigonal-bipyramidal, with a trigonality index, τ, of 0.51.[25] There is an extended network of hydrogen bonds between the hexanuclear clusters, in particular: 1) there are quite strong hydrogen bonds between the two hydrogen atoms at O8 and the sulfite oxygens O11 and O13 (Figure 2, Table 4), thus forming a hydrogen-bonded layer of adjacent anions lying in the *ab* plane (Figure 2), 2) the hydroxylic hydrogen atom HO(6) forms a weak hydrogen bond with the terminal O2 oxygen of an adjacent

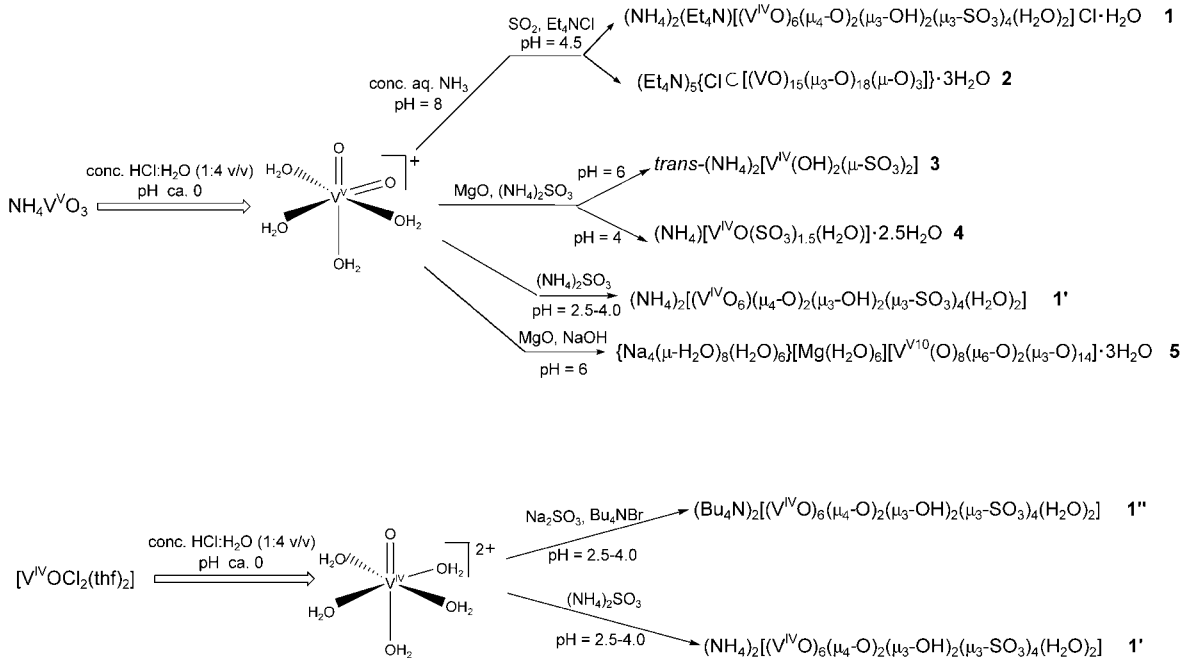

Scheme 1. Synthetic routes to isolated compounds **1**–**5**.

Table 1. Selected interatomic distances and angles relevant to the coordination sphere for the vanadium atoms in compound **1**.

		bond lengths [Å]			
V1–O1	1.607(3)	V2¦.25*ex*–O12	2.044(3)	V4¦.25*ex*–O4	1.593(3)
V1–O5	1.995(2)	V3¦.25*ex*–O3	1.591(3)	V4¦.25*ex*–O5	2.328(2)
V1–O6	2.299(3)	V3¦.25*ex*–O5	1.983(2)	V4¦.25*ex*–O6	2.008(2)
V1–O9	2.044(2)	V3¦.25*ex*–O8	2.065(3)	V4¦.25*ex*–O7	2.001(2)
V2–O2	1.603(3)	V3¦.25*ex*–O10	1.956(3)	V4¦.25*ex*–O11	2.030(3)
V2–O5	1.990(2)	V3¦.25*ex*–O13	1.966(3)	V4¦.25*ex*–O14	2.014(3)
V2–O7	2.317(3)				
		bond angles [°]			
O1-V1-O6	175.56(16)	O10-V3-O13	131.66(12)	O4-V4-O7	103.21(14)
O5-V1-O9A	155.84(10)	O3-V3-O10	114.42(14)	O4-V4-O11	98.23(12)
O5-V1-O9	90.23(9)	O3-V3-O13	112.35(14)	O4-V4-O14	98.03(12)
O5-V1-O5A	83.47(13)	O5-V3-O3	102.69(12)	O5-V4-O6	78.08(10)
O9-V1-O9A	86.05(13)	O5-V3-O10	90.49(10)	O5-V4-O7	78.45(11)
O1-V1-O5	104.23(12)	O5-V3-O13	90.77(10)	O5-V4-O11	80.13(9)
O1-V1-O9	99.93(12)	O8-V3-O3	94.68(12)	O5-V4-O14	81.87(9)
O2-V2-O7	174.12(16)	O8-V3-O10	79.89(10)	V1-O5-V2	94.91(9)
O5-V2-O12A	155.84(10)	O8-V3-O13	84.89(11)	V1-O5-V3	119.10(11)
O5-V2-O12	89.60(9)	O4-V4-O5	178.34(12)	V1-O5-V4	100.41(9)
O5-V2-O5A	83.76(13)	O6-V4-O14	157.52(12)	V2-O5-V3	118.96(11)
O12-V2-O12A	87.03(14)	O7-V4-O11	156.62(11)	V2-O5-V4	100.53(9)
O2-V2-O5	105.33(12)	O4-V4-O6	102.30(13)	V3-O5-V4	118.55(10)
O2-V2-O12	98.83(12)	O4-V4-O7	103.21(14)	V1-O6-V4	101.00(10)
O7-V2-O5	78.94(9)	O4-V4-O11	98.23(12)	V4-O6-V4A	102.79(14)
O7-V2-O12	76.98(9)	O4-V4-O14	98.03(12)	V2-O7-V4	100.58(11)
O5-V3-O8	162.44(10)	O4-V4-O6	102.30(13)	V4-O7-V4A	103.30(15)

hexanuclear cluster (Figure 2, Table 4) stabilising the hydrogen-bonded anionic layer, and 3) the hydroxylic hydrogen atom, HO(7) is involved in an interaction with the Cl^- counter-ion together with hydrogens from ammonium cations. The hexanuclear $V^{IV}\leftarrow[V_4^{IV}(\mu_4\text{-}O)_2(\mu_3\text{-}OH)_2]\rightarrow V^{IV}$ cluster represents a novel structural motif.[26,27]

The X-ray structure of **2** (Figure 3) exhibits a spherical $\{Cl\subset[(V^VO)_8(V^{IV}O)_7(\mu_3\text{-}O)_{18}(\mu\text{-}O)_3]\}^{5-}$ cluster, which formally contains eight V^V and seven V^{IV} centres arranged on the surface of a sphere at a distance of 3.45 ± 0.1 Å from the centre of the cluster in which the Cl^- resides.

Compound **3** has a linear polymeric structure (Figure 4). The crystallographically unique vanadium atom of compound **3** exhibits an octahedral geometry defined by four equatorial sulfite oxygen atoms and two axial hydroxo groups. The four equatorial V–O bonds are equivalent and equal to 1.996(4) Å, while the two axial V–O bonds are also equivalent and equal to 1.988(8) Å, which is somewhat longer than expected. Owing to the symmetry, the O3′-V1-O3 and O1-V1-O1″ angles are 180°, whereas the O1-V1-O1B and O1-V1-O3 angles are 91.5(3)° and 91.9(2)°, respectively, indicating almost an ideal octahedral geometry. The vanadium octahedra are linked together through four μ_2-pyramidal-sulfite bridges in 1D chains along the *c* axis. The μ_2-sulfite bridges exhibit an O1A-S1-O1 angle of 100.8(4)° and keep the vanadium octahedra in close proximity. The ammonium ions between the chains promotes stable packing. The hydrogen atoms of the ammonium group make two different close contacts with O2 oxygen

Table 2. Selected interatomic distances and angles relevant to the coordination sphere for the vanadium atoms for the compound **2**.

	Bond lengths [Å]		
V1−O1	1.588(4)	V5−O5	1.604(4)
V1−O34	1.862(4)	V5−O36	1.741(4)
V1−O24	1.897(4)	V5−O22	1.893(3)
V1−O19	1.901(4)	V5−O23	1.894(3)
V1−O16	2.012(4)	V5−O18	2.108(4)
V1−V6	2.8740(14)	V5−V6	3.0202(14)
V1−V2	2.8849(15)	V6−O6	1.598(4)
V2−O2	1.595(4)	V6−O16	1.863(4)
V2−O16	1.886(4)	V6−O18	1.889(4)
V2−O17	1.901(4)	V6−O24	1.913(4)
V2−O19	1.907(4)	V6−O23	1.939(4)
V2−O20	1.925(4)	V6−V15	2.9965(14)
V2−V3	2.9132(14)	V7−O7	1.593(4)
V2−V13	2.9692(14)	V7−O34	1.769(4)
V3−O3	1.595(4)	V7−O33	1.899(4)
V3−O35	1.853(4)	V7−O28	1.902(4)
V3−O21	1.895(4)	V7−O25	2.091(4)
V3−O20	1.902(4)	V7−V8	2.9704(14)
V3−O17	2.016(4)	V7−V12	3.0149(15)
V3−V4	2.9101(14)		
V4−O4	1.605(4)		
V4−O17	1.866(4)		
V4−O18	1.875(4)		
V4−O22	1.923(4)		
V4−O21	1.926(4)		
V4−V5	2.9906(14)		
V4−V14	3.0075(13)		
	Bond angles [°]		
O1-V1-O34	102.9(2)	V6-V1-V2	76.53(4)
O1-V1-O24	111.3(2)	O2-V2-O16	108.09(19)
O34-V1-O24	90.17(17)	O2-V2-O17	107.4(2)
O1-V1-O19	111.1(2)	O2-V2-O19	107.8(2)
O34-V1-O19	88.82(16)	O16-V2-O19	84.59(16)
O24-V1-O19	136.62(16)	O2-V2-O20	106.66(19)
O1-V1-O16	102.5(2)	O16-V2-O20	145.02(16)
O34-V1-O16	154.65(16)	O17-V2-O20	83.59(16)
O24-V1-O16	81.37(16)	O19-V2-O20	81.27(15)
O19-V1-O16	81.37(15)	O2-V2-V1	112.62(17)
O1-V1-V6	110.62(16)	O16-V2-V1	43.98(11)
O34-V1-V6	128.07(13)	O17-V2-V1	125.67(12)
O24-V1-V6	41.25(11)	O19-V2-V1	40.68(11)
O19-V1-V6	113.18(11)	O20-V2-V1	116.64(11)
O16-V1-V6	40.18(11)	O2-V2-V3	111.86(16)
O1-V1-V2	110.43(18)	O16-V2-V3	125.22(12)
O34-V1-V2	126.62(12)	O17-V2-V3	43.49(12)
O24-V1-V2	113.56(11)	O19-V2-V3	115.66(12)
O19-V1-V2	40.84(11)	O20-V2-V3	40.13(11)
O16-V1-V2	40.60(11)	V1-V2-V3	134.75(4)

Table 3. Selected interatomic distances and angles relevant to the coordination sphere for the vanadium atoms for the compound **3**.

Bond lengths [Å]		Bond angles [°]	
V1−O1	1.996(4)	O3-V1-O1	91.9(2)
V1−O3	1.988(8)	O1-V1-O1B	91.5(3)
S1−O1	1.522(4)	O1-S1-O1D	100.8(4)
S1−O2	1.523(7)		

atoms of sulfite anions from neighbouring chains. This may be the reason why O2 appears disordered over two positions in the structure.

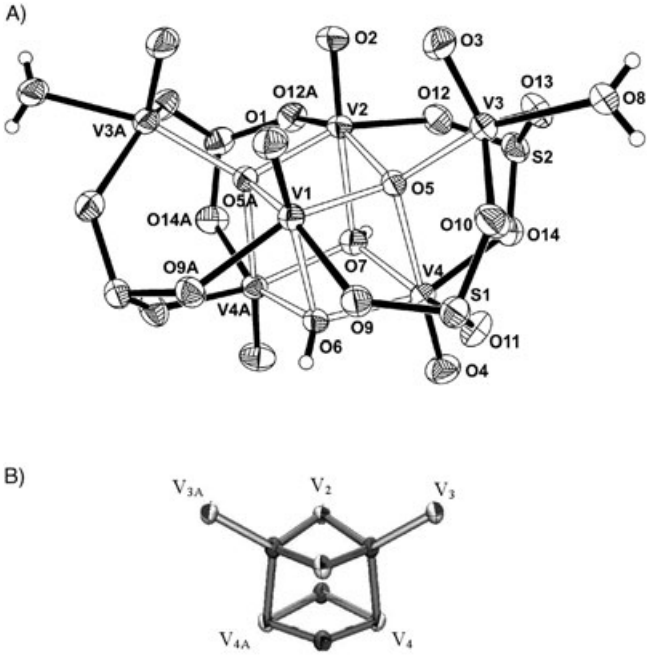

Figure 1. A) Structure of the complex anion $[(V^{IV}O)_6(\mu_4\text{-}O)_2(\mu_3\text{-}OH)_2(\mu_3\text{-}SO_3)_4(H_2O)_2]^{2-}$ from compound **1** (ORTEP diagram with 50% thermal ellipsoids). B) Representation of the magnetic model of **1**.

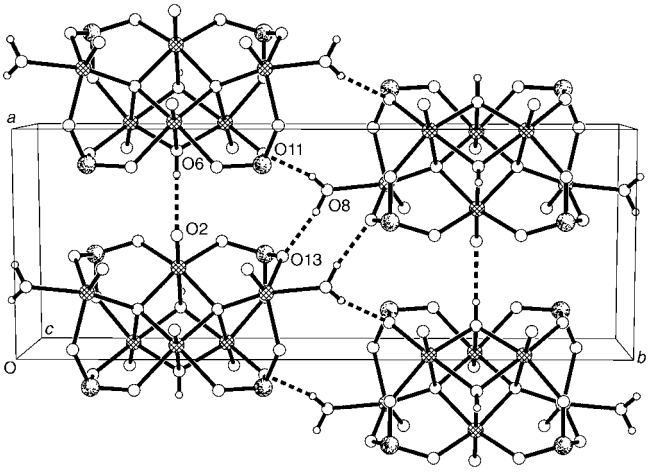

Figure 2. Packing diagram of compound **1** showing the hydrogen-bonded network; counterions and interstitial water molecules are not shown.

The two-dimensional structure of compound **4** is a layered net of VO_6 octahedra, each of which shares four corners with four adjacent sulfite trigonal pyramids. The connectivity between the VO_6 octahedra and the sulfite trigonal pyramids creates an open-framework compound with 8- and 4-ring windows (Figure 5). Compound **4** represents a rare example of an open-framework compound prepared under mild conditions (≈20 °C).[28]

The 2D structure of compound **5** can be described as a chain in which the edge-sharing octahedra of magnesium and sodium atoms are linked together in a zigzag conforma-

Table 4. Specified hydrogen bonds for compound **1**.

D–H	H···A	D···A	∢DHA	D–H···A
0.80	2.03	2.812(5)	165.6	O6–H6O···O2 ($x-1, y, z$)
0.82	2.30	3.117(4)	174.2	O7–H7O···Cl1 (x, y, z)
0.80	1.93	2.700(3)	162.4	O8–H1O8···O11 ($-x, -y+1, -z+1$)
0.81	1.93	2.706(3)	160.1	O8–H2O8···O13 ($-x+1, -y+1, -z+1$)
0.79	2.07	2.619(4)	127.1	O15–H1O5···O12 (x, y, z)
0.79	2.13	2.723(4)	131.9	O15–H1O5···O4 ($x+1, y, z$)
0.84	2.36	3.195(10	173.0	N2–H1N2···Cl1 ($x, y, z-1$)
0.85	1.78	2.613(12)	170.5	N2–H2N2···O15 ($x-1, y, z-1$)
0.86	2.30	3.161(4)	177.2	N3–H1N3···Cl1 ($x, y, z-1$)
0.85	2.27	2.937(4)	134.9	N3–H2N3···O9 ($x+1, y, z$)
0.86	2.21	3.036(5)	163.3	N3–H3N3···O1 (x, y, z)
0.85	2.37	2.872(4)	118.3	N3–H2N3···O3 (x, y, z)

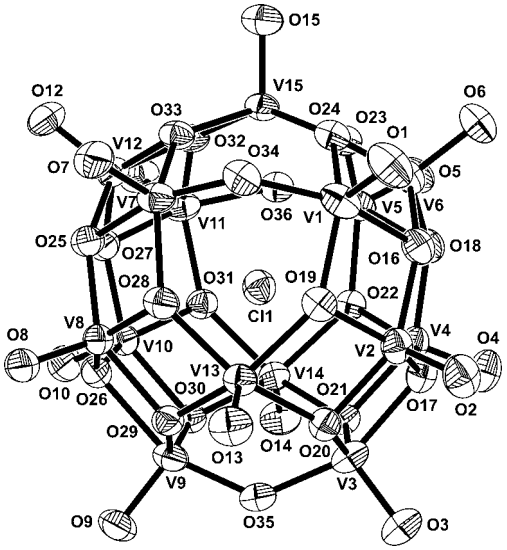

Figure 3. Structure of compound **2** (ORTEP diagram with 50% thermal ellipsoids), counter-cations and interstitial water molecules are not shown.

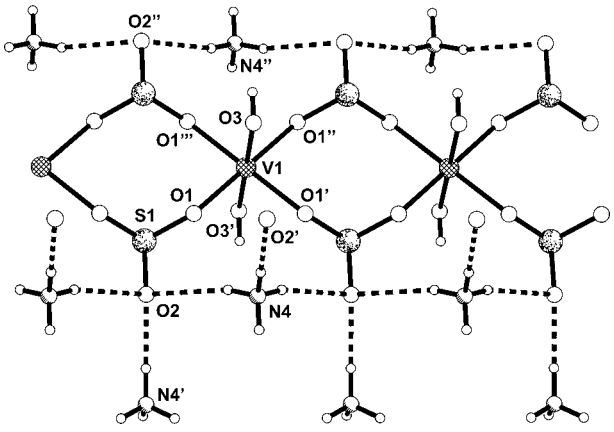

Figure 4. Ball-and-stick representation of compound **3** depicting the hydrogen-bonded network.

tion. Chains are inter-linked with decavanadate(v) clusters, which are connected to sodium atoms through μ-oxygen bridges (Figure 6).

IR spectroscopy: Assignments of some diagnostic bands for the vanadium(IV) sulfite compounds **1**, **3** and **4** as well as for some known metal-sulfite compounds are given in Table 5. One should expect the SO_3^{2-} bands of the compounds **1**, **3**, and **4** near the positions of the four fundamentals (ν_1–ν_4) of the pyramidal (C_{3V}) sulfite anion. The wavenumbers of the fundamentals of the free sulfite groups are well-known,[29] namely: $\nu_1(A_1) = 967\,cm^{-1}$, $\nu_2(A_1) = 620\,cm^{-1}$, $\nu_3(E) = 933\,cm^{-1}$, and $\nu_4(E) = 469\,cm^{-1}$, according to the IR spectra of aqueous sulfite sol-

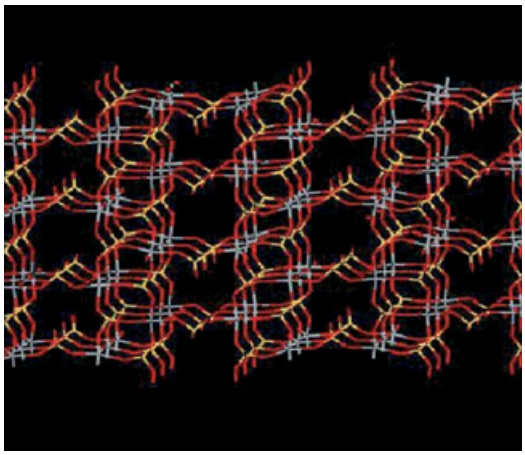

Figure 5. Packing diagram of compound **4** showing a 2D network (from ref. [16b]).

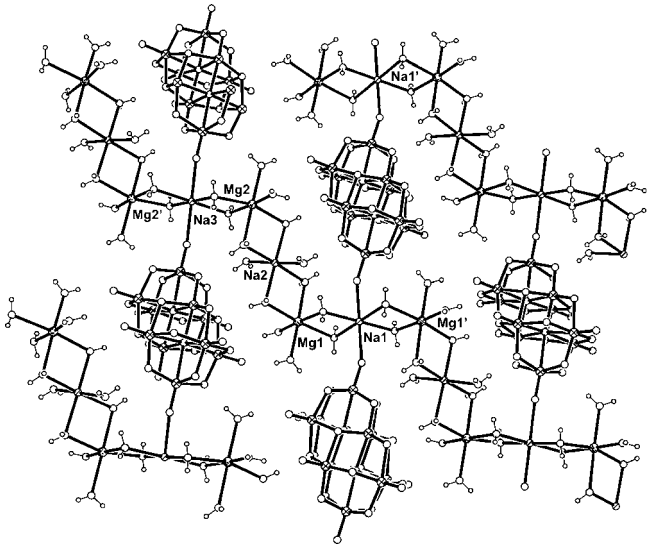

Figure 6. Packing diagram of compound **5** showing a 2D network; the isolated $[Mg(H_2O)_6]^{2+}$ ion and interstitial water molecules have been omitted for clarity.

Table 5. Diagnostic IR bands [cm^{-1}] of the vanadium(IV)-sulfite compounds **1**, **3**, **4** and of some known *O*- and *S*-bonded metal sulfite compounds.

Compound	Bonding modes[a] of SO_3^{2-}	ν_3(E)	ν_1(A_1)	$\Delta\lvert\nu_3-\nu_1\rvert$ [cm^{-1}]	ν_2(A_1) ν(V-OSO_2) ν(V-O-V)	ν_4(E)	ν(V=O)	ν(V-OH)	Ref.
1	μ_3-(*O*,*O*,*O*)		1014 s, 978 s[b] 940 s, 910 sh 904 s, 839 m	176	641 w, 585 s 561 s, 529 m 498 w, 457 w 441 w, 408 w		967 vs 960 vs		this work
3	μ-(*O*,*O*)		1028 vs, 1012 vs 979 vs, 952 vs 898 vs, 835 vs	193	553 m, 492 w			685 s	this work
4	μ_3-(*O*,*O*,*O*) and μ-(*O*,*O*)		1018 s, 993 sh 987 s, 966 sh, 903 s, 841 m	177	646 w, 591 m 563 m, 535 m 490 w, 424 w		952 vs		this work
cis-$Na[Co^{III}(SO_3)_2(en)_2]$	η^1-*S*	1095 s	943 vs	152	625 s				[45]
trans-$Na[Co^{III}(SO_3)_2(en)_2]$	η^1-*S*	1068 s	939 vs	129	630 s				[45]
$Tl_2[Cu(SO_3)_2]$	η^1-*O*	894 s, 860 s	981 s	127	670 w	498 m, 453 m			[46]
$Cu^{II}[Cu^{I}SO_3]_2\cdot 2H_2O$	η^1-*O*	977 s, 912 m	1025 m	113	636 m	499 m, 480 m			[46]

[a] See Scheme 1. [b] Intensity codes: s = strong; m = medium; w = weak; sh = shoulder.

utions; ν_1 and ν_3 are stretching vibrations, whereas ν_2 and ν_4 are bending vibrations. However, coordination of the sulfite ions and interactions with other ions in the crystal lattice are expected to reduce the symmetry, shift the fundamentals and lift the degeneracy of the sulfite modes. An overlap between the V=O and SO stretches is expected for compounds **1** and **4** and between the V–O stretches and SO bendings for **1**, **3** and **4**, respectively. Because compound **3** does not possess a V=O bond, it is reasonable to assign the six strong peaks observed in the range 1028–835 cm^{-1} to SO stretching vibrations. The strong peak at 685 cm^{-1} of **3** was assigned to ν(V–OH) based on the absence of this peak in the spectra of the oxovanadium(IV)-sulfite compounds **1** and **4**. The V=O stretches of compounds **1** and **4** were observed as very strong bands at 967, 960 and 952 cm^{-1}, respectively. Although, the V=O stretches appear in the same region as the SO stretches, they were easy to identify because the V=O stretching vibrations have a larger intensity than the corresponding SO stretching vibrations. From Table 5, it is obvious that $\Delta\lvert\nu_3-\nu_1\rvert$, the difference between the highest and the lowest SO stretching vibrations in metal sulfite species, is substantially larger for the μ_2-*O*,*O* and μ_3-*O*,*O*,*O* (Scheme 2) coordination modes of SO_3^{2-} anion, for which this difference is $\approx$180 cm^{-1}, compared to either the η^1-*S* or η^1-*O* (Scheme 2) coordination modes for which this difference is $\approx$130 cm^{-1}. Thus, it is easy to distinguish the μ_2-(*O*,*O*) and μ_3-(*O*,*O*,*O*) coordination modes from the η^1-*S* (two peaks) and η^1-*O* (three peaks) modes because since the former have the following features: 1) six peaks in the range 1020–835 cm^{-1} and 2) $\Delta\lvert\nu_3-\nu_1\rvert\approx$180 cm^{-1}.

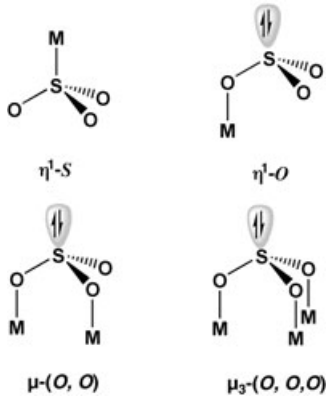

Scheme 2. The four coordination modes of the sulfite anion reported in Table 5.

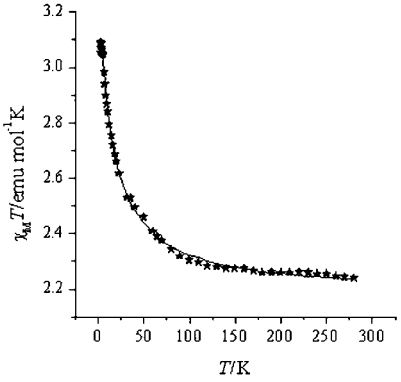

Figure 7. Temperature dependence of the susceptibility of compound **1**.

Magnetic studies: The experimental magnetic data for **1** are given as a plot of $\chi_M T$ versus T in Figure 7. The $\chi_M T$ value increases from 2.24 emu $mol^{-1}K^{-1}$ at 300 K, which is in perfect agreement with the expected value of 2.25 emu $mol^{-1}K^{-1}$ for six non-interacting V^{IV} centres (S = $^1/_2$), to 3.1 emu $mol^{-1}K^{-1}$ at 2 K. The increase of $\chi_M T$ with decreasing temperature suggests the existence of ferromagnetic exchange interactions within the molecule. The Hamiltonian formalism used to fit the experimental data for this V_6^{IV} system (Figure 1B) is given by Equation (1).

$$\begin{aligned} H &= J_1(S_{4A}S_4) + J_2(S_1S_2) + J_3[S_{4A}(S_1+S_2) \\ &\quad + S_4(S_1+S_2)] + J_4[S_3(S_1+S_2+S_4) \\ &\quad + S_{3A}(S_1+S_2+S_{4A})] \end{aligned} \qquad (1)$$

Equation (1) gave a very good fit (solid line in Figure 7) and the following values: $J_1 = 2.0\,cm^{-1}$, $J_2 = -47.0\,cm^{-1}$, $J_3 = -5.0\,cm^{-1}$, $J_4 = 1.0\,cm^{-1}$, $g = 1.97$. This fit reveals the existence of two ferromagnetic exchange parameters within the V_6^{IV} cluster. The first one is between the V1 and V2 atoms (Figure 1B) (V···V 2.936(1) Å; av V-O-V 94.9(1)°) and the second one is between the V4A and its symmetry-related V4 and V1/V2 atoms, which are also symmetry-related, (V···V 3.331(2) Å; av V-O-V 100.5(1)°). Antiferromagnetic interactions are expected between the V4 and V4A centres (V···V 3.138(3) Å; av V-O-V 103.0 (1)°) and between the V3 and V1/V2 atoms as well as its symmetry-related V3A and V1/V2, (V···V 3.429(2) Å, av V-O-V 109.0 (1)°). In general, the antiferromagnetic behaviour is the most common feature in oxovanadium(IV) clusters.[30a,b] The existence of ferromagnetic interactions is quite surprising and possibly involves the phenomenon of accidental orthogonality.[30c]

An examination of the literature indicated that the vanadium(IV) ion shows analogous magnetostructural correlations to the copper ion. In order not to increase the number of fitting parameters in the above model, we included in the J_4 constant the exchange interaction of the V3 with the V4 and the V3A with V4A (V···V 3.624(2) Å; av V-O-V 114.7 (1)°). The energy diagram is shown in Figure 8, where the ground

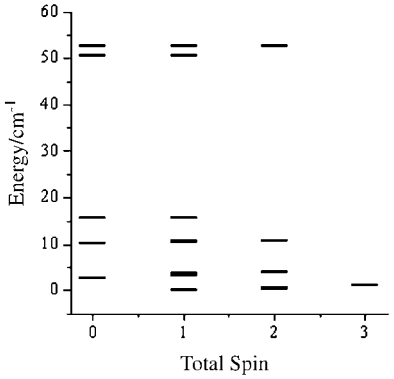

Figure 8. Energy representation of the ground and excited states of compound **1**.

state of the system is a $S_T = 1$ and two different $S_T = 2$ excited states are at about 0.4 and 0.7 cm^{-1}, respectively, while the $S = 3$ excited state is at 1 cm^{-1}. To verify the above fitting parameters, variable-field magnetisation data were collected at two different temperatures, 2.5 and 5.0 K. The data are plotted as $M/N\mu_B$ versus H/T in Figure 9 (where N is Avogadro's number and μ_B is the Bohr magneton). On account of the large number of fitting parameters used to fit the susceptibility data, the same magnetic model was used to simulate the magnetisation data with the exchanged constants fixed to the above-mentioned values. The results (solid lines in Figure 9) are in perfect agreement with the experimental data.

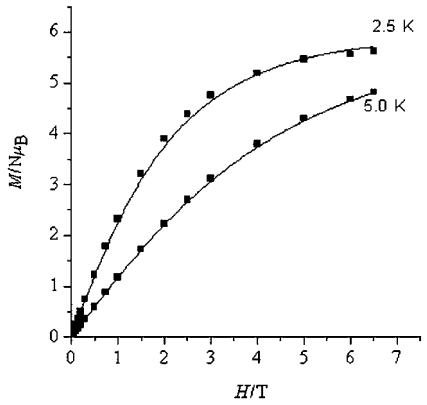

Figure 9. Simulation of the magnetisation data at $T = 2.5$ and 5.0 K.

The $\chi_M T$ and χ_M data versus temperature for compound **3** are shown in Figure 10. The $\chi_M T$ value, of 0.33 emu mol^{-1} K^{-1} at room temperature is in agreement

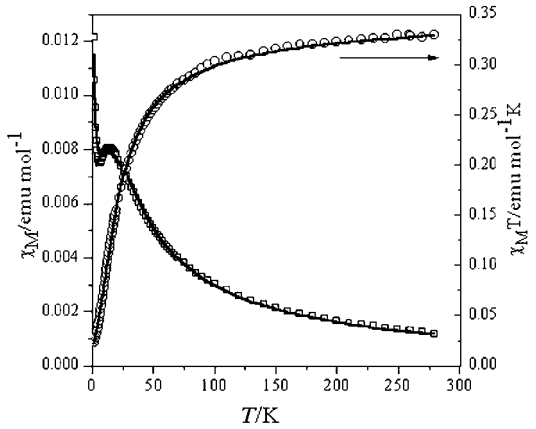

Figure 10. Temperature dependence of the susceptibility of compound **3**.

with the expected value of 0.375 for one isolated V^{IV} centre ($S = 1/2$) and decreases slowly until $T = 75$ K to a value of 0.28 and then more rapidly to a value close to zero at 2 K. This behaviour is indicative of an antiferromagnetic exchange interaction between the vanadium centres in compound **3**. The 1D character of the system is revealed in the χ_M versus T curve, where the χ_M value increases as the temperature decreases until $T = 14$ K (the χ_M maximum is 0.008 emu mol^{-1}). Below this temperature, the χ_M value decreases to about 6 K and then increases again owing to a paramagnetic impurity with $S = 1/2$. Bonner and Fisher have shown that the position of the maximum in the antiferromagnetic susceptibility can be estimated by the equations $kT_{max}/|J| \approx 1.282$ and $|J|\chi_{max}/g^2\beta^2N \approx 0.0735$. According to these equations, $|J| = 7.56\,cm^{-1}$, $g = 1.80$. The reason for the low g value is probably the paramagnetic impurity, which is important for $T < 15$ K. Over the entire temperature range, the data are best fit by the Bonner–Fisher

model[31,32] [Eq. (2)] for a uniformly spaced chain of $S = {}^1/_2$ metal centres, with a paramagnetic impurity correction (ρ).

$$\chi = (1-\rho)\frac{Ng^2\beta^2}{kT}\frac{0.25 + 0.07497\chi + 0.075235\chi^2}{1.0 + 0.9931\chi + 0.172135\chi^2 + 0.757825\chi^3} + \rho\frac{Ng^2\beta^2 S(S+1)}{3kT} \quad (2)$$

In Equation (2), $\chi = \frac{|J|}{kT}$. The fit (solid lines in Figure 10) gave $|J| = 9.65\,\mathrm{cm}^{-1}$, $g = 1.93$, and $\rho = 3.85\,\%$. The $|J|$ values obtained from these two different approaches are close to each other, whereas a more reasonable g value was obtained from the second method in which a paramagnetic impurity parameter (ρ) was introduced. The experimental magnetic data, where the $\chi_M T$ value at room temperature is in agreement with the expected value for an isolated V^{IV} centre as well as the obtained fit, which revealed the existence of a weak antiferromagnetic exchange interaction between the vanadium centres in the polymer, confirm that the oxidation state of the metal is +IV. Variable-field magnetisation data, M versus H, were collected at $T = 2\,\mathrm{K}$ and in the field range 0–12 T (Figure 11).

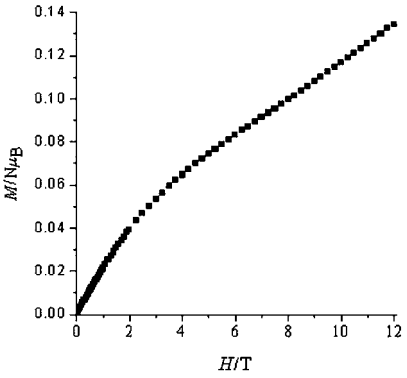

Figure 11. Field dependence of the magnetisation at 2 K in the field range 0–12 T.

The magnetisation does not saturate at 12 T, and this is indicative of antiferromagnetically coupled spins. The sigmoid form of the magnetisation curve comes from the contribution of the paramagnetic impurity of a system with $S = {}^1/_2$ plus the presence of a spontaneous moment attributed to the presence of canted spins, something that has already been reported for other 1D $S = {}^1/_2$ systems.[33]

The μ_{eff} of **2** at room temperature is 3.2 μ_B, which is substantially less than the theoretical value of 4.58 μ_B for seven non-interacting V^{IV} centres ($S = {}^1/_2$) (Table 6). The V···V distances in compound **2** are in the range of 2.816(1)–3.020(1) Å, thus indicating spin–spin interactions. At this point, it is worth noting that the other two [Cl⊂V_{15}] clusters reported in the literature, namely: $\{Cl\subset[(V^{V}O)_7(V^{IV}O)_8(\mu_3\text{-}O)_8(\mu\text{-}O)_3]\}^{6-}$ (**2′**),[23] and $\{Cl\subset[(V^{V}O)_9(V^{IV}O)_6(\mu_3\text{-}O)_8(\mu\text{-}O)_3]\}^{4-}$ (**2″**)[24] have V···V distances in the range of 2.93–3.00 and 2.83–3.05 Å, respectively. Their experimental μ_{eff} values are 3.9 and 2.35 μ_B for **2′** and **2″** and the theoretical μ_{eff} values for eight and six non-interacting V^{IV} centres ($S = {}^1/_2$) are 4.90 and 4.24 μ_B, respectively (Table 6). From all this data, it is evident that the spin–spin interactions of the V^{IV} centres increase as the negative charge of the clusters decreases, whereas there is no apparent correlation between the vanadium···vanadium distances and the experimental μ_{eff} values.

Table 6. Comparison of $\mu_{eff}^{exp/theor}$ values, $\Delta\mu_{eff}$ values and vanadium–vanadium distances in the {Cl⊂[V_{15}]} clusters.

Cluster	μ_{eff}[μ_B][b]	μ_{eff}[μ_B][c]	$\Delta\mu_{eff}$[d]	V···V range [Å]	Ref.
$\{Cl\subset[(VO)_{15}(\mu_3\text{-}O)_{18}(\mu\text{-}O)_3]\}^{6-}$ $[V_7^{V}V_8^{IV}]$[a]	3.90	4.90	1.00	2.93–3.00	[23]
$\{Cl\subset[(VO)_{15}(\mu_3\text{-}O)_{18}(\mu\text{-}O)_3]\}^{5-}$ $[V_8^{V}V_7^{IV}]$	3.20	4.58	1.38	2.82–3.02	this work
$\{Cl\subset[(VO)_{15}(\mu_3\text{-}O)_{18}(\mu\text{-}O)_3]\}^{4-}$ $[V_9^{V}V_6^{IV}]$	2.35	4.24	1.89	2.83–3.03	[24]

[a] The decapentanuclear cluster $[(V^{V}O)_7(V^{IV}O)_8(\mu_3\text{-}O)_{18}(\mu\text{-}O)_3]^{5-}$,[27] which does not encapsulate a Cl^-, has an experimental μ_{eff} value of 2.86 μ_B. [b] Experimental value at room temperature. [c] Theoretical values for eight, seven and six non-interacting V^{IV} centres ($S = {}^1/_2$), respectively. [d] $\Delta\mu_{eff} = \mu_{eff}^{theor} - \mu_{eff}^{exp}$.

Theoretical calculations of 3: The geometry of compound **3** has been also investigated by means of open-shell density functional calculations. It is very difficult to carry out such calculations on the polymeric structure of compound **3**. Thus, to simulate the polymeric structure, the theoretical study was undertaken on the basis of two model species $[(SO_3)_2V^{IV}(OH)_2(\mu\text{-}SO_3)_2V^{IV}(OH)_2(SO_3)_2]^{8-}$ (**3a**) and $[(SO_3)_2V^{IV}(OH)_2(\mu\text{-}SO_3)_2V^{IV}(OH)_2(\mu\text{-}SO_3)_2V^{IV}(OH)_2(SO_3)_2]^{10-}$ (**3b**) in which two and three *trans*-$[V^{IV}(OH)_2]^{2+}$ units, respectively, are bridged to each other by two μ_2-SO_3^{2-} groups (Figure 12). The spin multiplicity was 3 and 4 for **3a** and **3b**, respectively. A partial optimisation of the geometry of the two models was carried out in which the $[V^{IV}(OH)_2(\mu\text{-}SO_3)_2\text{-}V^{IV}(OH)_2]$ or the $[V^{IV}(OH)_2(\mu\text{-}SO_3)_2V^{IV}(OH)_2(\mu\text{-}SO_3)_2V^{IV}\text{-}(OH)_2]^{2-}$ cores were fully optimised. Bond lengths within the four terminal SO_3^{2-} ligands were also optimised, but the bond and torsion angles were kept constant. Thus, whereas the two cores were allowed to breath freely, the orientation of the terminal SO_3^{2-} ligands was kept fixed to resemble the SO_3^{2-} ligands in the polymeric structure of compound **3**.

The final optimised geometries of the **3a** and **3b** model species are depicted in Figure 12, and selected calculated structural parameters are reported in Table 7. There is no great difference between the overall geometries of the binuclear and trinuclear cores. In general, and taking into account that the models are simplified, one can observe a satisfactory agreement between the calculated and the experimental values of the geometrical parameters. Bond lengths

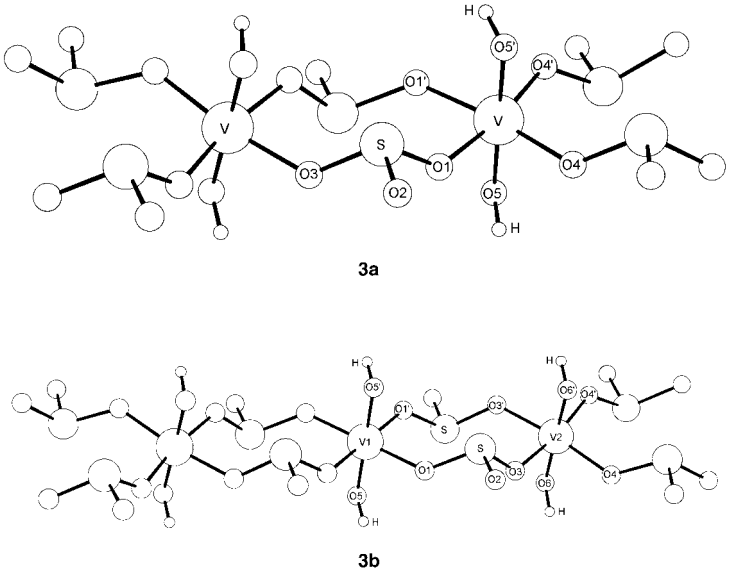

Figure 12. Final optimised geometries of the model complexes **3a** and **3b**.

agree within 0.06 Å, while the largest deviation of the bond angles appears to be about 8°. The greatest discrepancy concerns the longer V···V non-bonding distance calculated to be 5.379 Å and 5.261 Å for **3a** and **3b**, respectively. However, as this distance is shorter in the trinuclear model species, we can safely assume that it would be closer to the experimental V···V value of 5.13 Å in a calculation of a larger model species. Thus, it can be concluded that the polymeric structure of **3** is well modelled by the binuclear or trinuclear model species.

Table 7. Selected bond lengths [Å] and bond angles [°] calculated for the model compounds **3a** and **3b**.[a]

	3a		**3b**
V–O1	2.018	V1–O1	2.015
		V2–O3	1.996
V–O4	2.042	V2–O4	2.054
V–O5	1.985	V1–O5	1.985
		V2–06	1.988
V···V	5.379	V1···V2	5.261
S–O1	1.570	S–O1	1.581
S–O2	1.561	S–O2	1.559
S–O3	1.570	S–O3	1.574
O5–H	0.985	O5–H	0.982
		O6–H	0.983
O1-V-O1′	85.7	O1-V1-O1′	86.5
		O3-V2-O3′	82.3
O4-V-O4′	101.4	O4-V2-O4′	100.3
O5-V-O5′	179.6	O5-V1-O5′	180.0
		O6-V2-O6′	179.6
O1-S-O2	103.8	O1-S-O2	103.2
O2-S-O3	103.9	O2-S-O3	104.3
O1-S-O3	102.3	O1-S-O3	103.0
V-O5-H	104.0	V1-O5-H	105.2
		V2-O6-H	103.8

[a] Numbering scheme as in Figure 1.

In the optimised structures, the calculated value of the spin operator $<S^2>$ was 2.005 for **3a** and 3.751 for **3b**. The calculated Mulliken atomic spin densities for the vanadium atoms in **3a** were 1.085, 1.089 and 1.104 for V1 and V2/V2′, respectively in **3b**. According to the results of the spin population analysis, the two models should be considered as binuclear d^1–d^1 or trinuclear d^1–d^1–d^1 systems.

According to Hoffmann's model for superexchange interactions in polynuclear complexes bridged by polyatomic ligands, the degenerate d-orbital combinations of the metal fragments interact with symmetry-appropriate orbitals of the bridging ligands to result in the SOMOs of the complex. The extent of the superexchange interaction depends on the degree of delocalisation of the SOMOs over the intervening bridging atoms and on the energy gap between the SOMOs, with the latter closely related to the absolute magnitude of the antiferromagnetic term, J_{AF}, of the superexchange interaction.[34] The shapes of the two highest singly occupied molecular orbitals (SOMOs) of **3a** and of the three SOMOs of **3b** are presented in Figure 13. Each of the SOMOs is local-

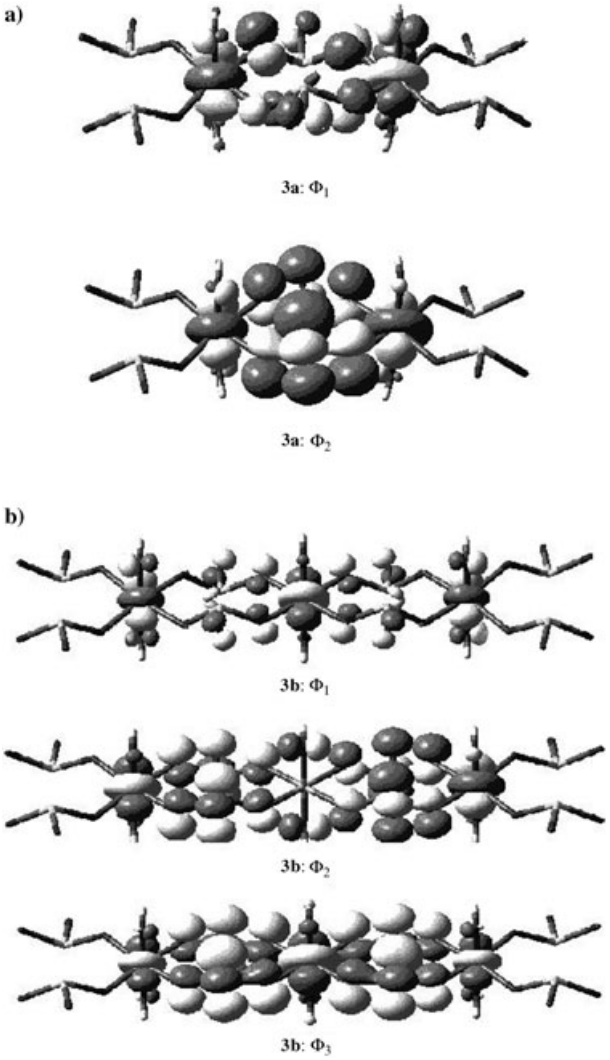

Figure 13. Shapes of the SOMOs, Φ_1 and Φ_2 of the model complex **3a** (a) as well as Φ_1, Φ_2 and Φ_3 SOMOs of the model complex **3b** (b) (small contributions from orbitals of the SO_3^{2-} terminal ligands are not shown for clarity).

ised to the d orbitals of the V^{IV} atoms with significant participation from orbitals of the intervening atoms of the SO_3^{2-} bridging ligands. However, the ligand orbitals are always orthogonal to the metal d orbitals. This situation is ideal to observe the phenomenon of accidental orthogonality and a small antiferromagnetic interaction. This is in agreement with the experimentally observed value of the effective magnetic moment of the complex, which is typical of weakly electron-coupled vanadium(IV) ($S = {}^1/_2$) centres.

Conclusion

A series of unprecedented vanadium(IV) sulfite compounds was synthesised by reacting NH_4VO_3 with either sulfur dioxide (compound **1**) or ammonium sulfite in the presence of *magnesium oxide* (compounds **3** (pH 4) and **4** (pH 6)). The host–guest cluster $(Et_4N)_5\{Cl\subset[(VO)_{15}(\mu_3\text{-}O)_{18}(\mu\text{-}O)_3]\}\cdot 3H_2O$ (**2**) was formed along with crystals of compound **1**. The solid-state molecular structures of compounds **1**–**4** were determined by single-crystal X-ray structure analysis. The hexanuclear oxovanadium(IV) sulfite cluster, $(NH_4)_2(Et_4N)[(V^{IV}O)_6(\mu_4\text{-}O)_2(\mu_3\text{-}OH)_2(\mu_3\text{-}SO_3)_4(H_2O)_2]Cl\cdot H_2O$ (**1**), exhibits a unique structural motif, consisting of a distorted cubane unit, $[V_4^{IV}(\mu_4\text{-}O)_2(\mu_3\text{-}OH)_2]$, connected to two outer vanadium(IV) atoms through two $\mu_4\text{-}O^{2-}$ and four $\mu_3\text{-}SO_3^{2-}$ bridges. The temperature dependence of the magnetic susceptibility data for compound **1** revealed an overall ferromagnetic behaviour, which is unprecedented for V^{IV} clusters. The non-oxo-vanadium(IV) sulfite species, *trans*-$(NH_4)_2[V^{IV}(OH)_2(\mu\text{-}SO_3)_2]$ (**3**), is a unique example of a bare vanadium(IV) species in which an oxidizing (V^{IV}) and reducing agent (SO_3^{2-}) coexist. Variable-temperature magnetic susceptibility measurements and theoretical studies for compound **3** verified that the oxidation state of vanadium is IV. Compound $(NH_4)[V^{IV}O(SO_3)_{1.5}(H_2O)]\cdot 2.5H_2O$ (**4**), the oxovanadium(IV) sulfite species, represents a rare example of an open-framework compound isolated under mild conditions. Efforts to prepare new polyoxometal sulfite clusters by variation of temperature, pressure, counterions and pH are underway.

Experimental Section

Materials: Reagent-grade chemicals were obtained from Aldrich, and used without further purification. C, H, N and S analyses were conducted by the microanalytical service of the University of Manchester. Vanadium was determined gravimetrically as vanadium pentoxide.

$(NH_4)_2(Et_4N)[(V^{IV}O)_6(\mu_4\text{-}O)_2(\mu_3\text{-}OH)_2(\mu_3\text{-}SO_3)_4(H_2O)_2]Cl\cdot H_2O$ (1), $(Et_4N)_5\{Cl\subset[(VO)_{15}(\mu_3\text{-}O)_{18}(\mu\text{-}O)_3]\}\cdot 3H_2O$ (2): Solid NH_4VO_3 (0.60 g, 5.1 mmol) was dissolved in aqueous HCl (37% HCl in water, 1:4 v/v, 20 mL, pH ≈ 0). The pH of the solution was adjusted to 8.5 by addition of concentrated aqueous ammonia. Subsequently, SO_2 was bubbled into the solution for about 15 min. The orange-red colour of the solution progressively changed to deep green and the final pH of the solution was about 4.5. Solid Et_4NCl (1.00 g, 6.0 mmol) was added, and the solution was stirred for 15 min. The precipitate was removed by filtration and the filtrate left in an open vessel at room temperature (≈20 °C) for four days, during which time light blue needle-shaped crystals of **1** as well as dark green crystals of **2**, suitable for single-crystal X-ray structure analysis, were formed. The crystals were filtered and dried in air. The crystals of compounds **1** and **2** were separated manually.

Complex ***1***: Yield: 1.19 g (38%); elemental analysis calcd (%) for $C_8H_{36}ClN_3O_{25}S_4V_6$ (1043.73): C 9.21, H 3.48, N 4.03, S 12.29, V 29.28; found: C 9.31, H 3.61, N 4.14, S 12.30, V 28.92; UV/Vis (H_2O): λ (ε [$M^{-1}cm^{-1}$]) = 236 (33400), 868 (203) nm.

Complex ***2***: Yield: 0.10 g (13%); elemental analysis calcd (%) for $C_{40}H_{106}ClN_5O_{39}V_{15}$ (2080.85): C 23.07, H 5.09, N 3.36, V 36.76; found C 23.14, H 5.13, N 3.35, V 36.54; UV/Vis (H_2O): λ (ε [$M^{-1}cm^{-1}$]) = 246 (7600), 889 (45 100) nm.

***trans*-$(NH_4)_2[V^{IV}(\mu\text{-}SO_3)_2(OH)_2]$ (3)**: Solid MgO (0.59 g, 14.6 mmol) was added slowly to a stirred solution of NH_4VO_3 (0.60 g, 5.1 mmol) in aqueous HCl (37% HCl in water, 1:4 v/v, 20 mL, pH ≈ 1). Subsequently, solid $(NH_4)_2SO_3$ (6.00 g, 61.2 mmol) was slowly added in small portions. In the pH range ≈2.6–3, a precipitate sometimes was formed that redissolved upon further addition of $(NH_4)_2SO_3$. When the whole quantity of $(NH_4)_2SO_3$ was added to the solution, its colour changed from blue to dark green and its pH value was 6. The reaction mixture was stirred for 15 min and then filtered. The filtrate was left to crystallise at room temperature in an open vessel for four days. Square platelike light green crystals were filtered and dried in air. Yield: 0.80 g (56%, based on vanadium); elemental analysis calcd (%) for $H_{10}N_2O_8S_2V$ (281.16): H 3.58, N 9.96, S 22.81, V 18.12; found H 3.63, N 10.21, S 22.66, V 17.81.

$(NH_4)[V^{IV}O(SO_3)_{1.5}(H_2O)]\cdot 2.5H_2O$ (4): Compound **4** was prepared in 45% yield in a manner similar to **3** from 4.50 g (45.9 mmol) of $(NH_4)_2SO_3$ instead of 6.00 g (61.2 mmol). Upon addition of $(NH_4)_2SO_3$, the colour of the reaction mixture turned blue and the final pH value was about 4. The solution was filtered and the filtrate was left crystallise for six days in an open vessel at room temperature. The blue hexagonal crystals were filtered and dried in air. Yield: 2.10 g (60%, based on vanadium); elemental analysis calcd (%) for $H_{11}NO_9S_{1.5}V$ (268.13): H 4.13, N 5.22, S 17.94, V 19.00; found: H 4.20, N 5.10, S 18.05, V 18.80.

$\{Na_4(\mu\text{-}H_2O)_8(H_2O)_6][Mg(H_2O)_6][V_{10}^{V}O_8(\mu_6\text{-}O)_2(\mu_3\text{-}O)_4(\mu\text{-}O)_{14}]\cdot 3H_2O$ (5): Solid MgO (0.59 g, 14.6 mmol) was added in one portion to a stirred solution of NH_4VO_3 (0.60 g, 5.1 mmol) in aqueous HCl (37% HCl in water, 1:4 v/v, 20 mL, pH ≈ 1). Solid NaOH (2.40 g, 60.0 mmol) was added to the reaction mixture and the final pH of the solution was about 6. The solution was filtered, and orthogonal orange crystals were obtained after one day by vapour diffusion of methyl alcohol into the filtrate. Yield: 2.00 g (26%, based on vanadium); elemental analysis calcd (%) for $H_{46}MgNa_4O_{49}V_{10}$ (1456): H 3.15, Na 6.31, Mg 1.64, V 35.02; found: H 3.23, Na 5.28, Mg 1.50, V 34.88; UV/Vis (H_2O): λ (ε [$dm^3mol^{-1}cm^{-1}$]) = 218 (65000), 241 (54200) nm.

X-ray crystallography: Crystals of compounds **1**, **2**, **3** and **5** were sealed in a glass capillary with the mother liquor to avoid decomposition of the crystals. Crystal data and details of data collection are listed in Table 8. Diffraction data were collected on a Bruker SMART 1 K 3-circle platform diffractometer equipped with a CCD detector. The frame data were acquired with the SMART[35] software and $Mo_{K\alpha}$ radiation (λ = 0.71073 Å). Final values of the cell parameters were obtained from least-squares refinement of the positions of all observed reflections. A total of 1271 frames were collected in three sets with a 0.3° ω-scan. The frames were then processed with the SAINT software[36] to give the *hkl* file corrected for Lorentz and polarisation effects. No absorption correction was applied. The structures were solved by direct methods with the SHELX-90[37] program and refined by least-squares method on F^2, SHELXTL-93,[36] incorporated in SHELXTL, Version 5.1.[39]

CCDC-233092 and CCDC-233440 contain the supplementary crystallographic data for this paper. These data can be obtained free of charge from The Cambridge Crystallographic Data Centre via www.ccdc.cam.ac.uk/data_request/cif.

Further details of the crystal structure investigations of compounds **3** and **5** can be obtained from the Fachinformationszentrum Karlsruhe, 76344 Eggenstein-Leopoldshafen, Germany, (fax: (+49) 7247-808-666; e-mail:

Table 8. Summary of crystallographic data for compounds **1**, **2**, **3** and **5**.

Compound	**1**	**2**	**3**	**5**
formula	$C_8H_{36}ClN_3O_{25}S_4V_6$	$C_{40}H_{106}ClN_5O_{39}V_{15}$	$H_{10}N_2O_8S_2V$	$H_{46}MgNa_4O_{28}V_{10}$
M_r	1043.73	2080.85	281.16	1488.04
a [Å]	7.621(1)	19.717(3)	6.543(1)	8.954(2)
b [Å]	19.780(3)	13.487(2)	13.393(2)	13.854(3)
c [Å]	11.666(2)	29.323(4)	5.130(1)	18.356(4)
α [°]	90	90	90	91.643(4)
β [°]	103.550(2)	94.131(2)	90	91.815(4)
γ [°]	90	90	90	104.442(4)
V [Å^3]	1709.7(4)	7777.6(17)	449.52(10)	2202.6(8)
Z	2	4	2	2
ρ_{calcd} [Mg m^{-3}]	2.027	1.777	2.077	2.244
space group	$P2_1/m$ (no. 11)	$P2_1/c$ (no. 11)	$Pnnm$ (no. 58)	$P\bar{1}$ (no. 1)
T [K]	298(2)	298(2)	301(2)	298(2)
λ [Å]	0.71073	0.71073	0.71073	0.71073
μ [mm^{-1}]	1.988	1.829	1.588	2.217
$R1$ (final)	0.0408	0.0548	0.0666	0.0264
$wR2$	0.1014	0.1336	0.1532	0.0650

crysdata@fiz.karlsruhe.de) on quoting the depository numbers CSD-413820 and CSD-413819

Physical measurements: IR spectra of the various compounds dispersed in KBr pellets were recorded on a Perkin-Elmer Spectrum GX FT-IR spectrometer. The temperature dependence of magnetic susceptibility was measured on polycrystalline powder samples with a cryogenics S600 SQUID Magnetometer for a applied field of 0.1 T and a temperature range of 2–300 K. Data were corrected for the contribution from the sample holder and diamagnetism of the sample by means of standard procedures.

Computational details: The electronic structure and geometry of the models studied were computed within the open-shell density functional theory. The hybrid B3LYP method was applied with Becke's three-parameter functional[40] and the non-local correlation is provided by the LYP expression.[41] The effective core potential (ECP) approximation of Hay and Wadt was used For V and S atoms, with the vanadium electrons described by the ECP being those of 1s, 2s and 2p shells, whereas the basis set used was of valence double-ζ quality.[42] The valence double-ζ basis set of Dunning and Huzinaga was used for the O and H atoms.[43] All calculations were performed with the Gaussian 98 package.[44]

Acknowledgements

N.L. thanks Dr. Claudio Sangregorio and the Department of Chemistry, Florence (Italy) for recording the magnetic measurements. We also thank Dr. A. Keramidas for his useful contribution to the IR discussion. This research was funded by the program "Heraklitos" of the Operational Program for Education and Initial Vocational Training of the Hellenic Ministry of Education under the 3rd Community Support Framework and the European Social Fund.

[1] a) M. T. Pope, A. Muller, *Angew. Chem.* **1991**, *103*, 56; *Angew. Chem. Int. Ed. Engl.* **1991**, *30*, 34; b) A. Muller, *Nature* **1991**, *352*, 115; c) C. L. Hill, guest editor, *Chem. Rev.* **1998**, *98*, 8; d) M. Farahbakhsh, H. Kagerler, H. Schmidt, D. Rehder, *Inorg. Chem. Commun.* **1998**, *1*, 111; e) A. Muller, M. T. Pope, F. Peters, D. Gatteschi, *Chem. Rev.* **1998**, *98*, 239; f) P. Gouzerh, R. Villaneau, R. Delmont. A. Proust, *Chem. Eur. J.* **2000**, *6*, 1184; g) V. Artero, A. Proust, P. Herson, P. Gouzerh, *Chem. Eur. J.* **2001**, *7*, 3901; h) V. Artero, A. Proust, P. Herson, F. Villain, C. Moulin, P. Gouzerh, *J. Am. Chem. Soc.* **2003**, *125*, 11156; i) T. Liu, E. Diemann, H. Li, A. Dress, A. Muller, *Nature* **2003**, *426*, 59.

[2] a) *Modular Chemistry* (Ed.: J. Michl), Kluwer Academic Publishers, Dordrecht, **1995**, and references threin; b) J. M. Clemente-Juan, E. Coronado, *Coord. Chem. Rev.* **1999**, *193–195*, 361; c) B. Saligngac, S. Riedel, A, Dolbecq, F. Secheresse, E. Cadot, *J. Am. Chem. Soc.* **2000**, *122*, 10381; d) J. P. Jolivet, *Metal Oxide Chemistry and Synthesis: From Solution to Solid State*, Wiley, New York, **2000**; e) E. Cadot, J. Marrot, F. Secheresse, *Angew. Chem.* **2001**, *113*, 796–799; *Angew. Chem. Int. Ed.* **2001**, *40*, 774; f) A. Dolbecq, C. Peloux, A. Auberty, S. Mason, P. Barboux, J. Marrot, E. Cadot, F. Secheresse, *Chem. Eur. J.* **2002**, *8*, 350; g) E. Cadot, J. Marrot, F. Secheresse, *J. Cluster Sci.* **2002**, *13*, 303.

[3] a) M. T. Pope, *Heteropoly and Isopoly Oxometalates*, Springer, New York, **1983**; b) A. Stein, S. W. Keller, T. E. Mallouk, *Science* **1993**, *259*, 1558; c) J. T. Rhule, C. L. Hill, D. A. Judd, *Chem. Rev.* **1998**, *98*, 327; d) H. Kwen, S. Tomlinson, E. Maata, C. Dablemont, R. Thouvenot, A. Proust, P. Gouzerh, *Chem. Commun.* **2002**, 2970; e) P. Mialane, L. Lisnard, A. Mallard, J. Marrot, E. Fidancev, P. Aschehoug, D. Vivien, F. Secheresse, *Inorg. Chem.* **2003**, *42*, 2102; f) J. Marrot, M. Pilette, F. Secheresse, E. Cadot, *Inorg. Chem.* **2003**, *42*, 3609; g) A. Muller, L. Toma, H. Bogge, M. Schmidtmann, P. Kogerler, *Chem. Commun.* **2003**, 2000.

[4] a) O. M. Yaghi, Li, H. Davis, C. Richardson, T. D. Groy, *Acc. Chem. Res.* **1998**, *31*, 474, and references therein; b) M. Eddaoudi, T. Moller, Li, H. Chen, B. T. Reineke, M. O'Keefe, O. M. Yaghi, *Acc. Chem. Res.* **2001**, *34*, 319, and references therein; c) J. Kim, B. Chen, T. Reineke, M. Eddaoudi, T. Moller, M. O'Keefe, O. M. Yaghi, *J. Am. Chem. Soc.* **2001**, *123*, 8239; d) A. Gaunt, I. May, R. Copping, A. Bhatt, D. Collison, D. Fox, T. Holman, M. Pope, *Dalton Trans.* **2003**, 3009; e) R. Rarig, J. Zubieta, *Dalton Trans.* **2003**, 1861; f) B. Modec, J. Brencic, E. Burkholder, J. Zubieta, *Dalton Trans.* **2003**, 4618.

[5] a) A. Gatteschi D. Gatteschi, R. Sessoli, P. Rey, *Acc. Chem. Res.* **1989**, *22*, 392; b) K. Nakatami, P. Bergerat, E. Codjovi, C. Mathoniere, Y. Pei, O. Kahn, *Inorg. Chem.* **1991**, *30*, 3977; c) K. Taft, C. Delfs, G. Papaefthymiou, S. Foner, D. Gatteschi, S. Lippard, *J. Am. Chem. Soc.* **1994**, *116*, 823.

[6] a) T. Yamase, *J. Chem. Soc. Dalton Trans.* **1985**, 2585; b) P. K. Bharadwaj, Y. Ohashi, Y. Sasaki, T. Yamase, *Acta Crystallogr. Sect. C* **1986**, *42*, 545; c) T. Yamase, M. Suga, *J. Chem. Soc. Dalton Trans.* **1989**, 661; d) T. Yamase, M. Sugata, E. Ishikawa, *Acta Crystallogr. Sect. C* **1996**, *52*, 1869; e) P. J. Hagrman, D. Hagrman, J. Zubieta, *Angew. Chem.* **1999**, *111*, 2798–2848; *Angew. Chem. Int. Ed.* **1999**, *38*, 2638–2684, and references therein.

[7] a) T. Ozeki, T. Yamase, H. Naruke, Y. Sasaki, *Inorg. Chem.* **1994**, *33*, 409; b) M. Sugeta, T. Yamase, *Acta Crystallogr. Sect. C* **1997**, *53*, 1166; c) B. E. Koene, N. J. Taylor, L. F. Nazar, *Angew. Chem.* **1999**, *111*, 3065–3068; *Angew. Chem. Int. Ed.* **1999**, *38*, 2888–2891.

[8] a) *Polyoxometalates: From Platonic Acids to Anti-retroviral Activity* (Eds.: M. T. Pope, A. Muller), Kluwer Academic Publishers: Boston, MA, **1994**; b) X. Wang, J. Liu, M. Pope, *Dalton Trans.* **2003**, 957.

[9] a) E. Heath, O. W. Howarth, *J. Chem. Soc. Dalton Trans.* **1981**, 1105; b) L. Petterson, B. Hedman, L. Anderson, N. Ingri, *Chem. Scr.* **1983**, *22*, 254; c) W. G. Klemperer, T. A. Marquart, O. M. Yaghi, *Angew. Chem.* **1992**, *104*, 51; *Angew. Chem. Int. Ed. Engl.* **1992**, *31*, 49; d) A. Muller, *J. Mol. Struct.* **1994**, *325*, 13; e) E. Burkholder, V. Golub, C. O'Connor, J. Zubieta, *Inorg. Chem.* **2003**, *42*, 6729; f) E. Burkholder, S. Wright, V. Golub, C. O'Connor, J. Zubieta, *Inorg. Chem.* **2003**, *42*, 7460.

[10] a) A. Muller, K. Mainzer, In *From Simplicity to Complexity - and Beyond* (Eds.: A. Muller, A. Dress, F. Vogtle), Vieweg, Braunschweig (Germany), **1996**, p. 1; b) C. Peloux, P. Mialane, A. Dolbecq, J. Marrot, F. Secheresse, *Angew. Chem.* **2002**, *114*, 2932–2934; *Angew. Chem. Int. Ed.* **2002**, *41*, 2808–2810; c) C. Peloux, A. Dolbecq, P. Mialane, J. Marrot, E. Riviere, F. Secheresse, *Inorg. Chem.* **2002**, *41*, 7100.

[11] a) M. T. Pope in *From Simplicity to Complexity - and Beyond* (Eds.: A. Muller, A. Dress, F. Vogtle), Vieweg, Braunschweig (Germany), **1996**, p. 137; b) K. Wassermann, M. H. Dickmann, M. T. Pope, *Angew. Chem.* **1997**, *109*, 1513–1516; *Angew. Chem. Int. Ed. Engl.* **1997**, *36*, 1445–1448.

[12] a) See reference [23]; b) A. Muller, M. Penk, E. Krickenmeyer, H. Bogge, H. J. Walberg, *Angew. Chem.* **1988**, *100*, 1787; *Angew. Chem. Int. Ed. Engl.* **1988**, *27*, 1719; c) A. Muller, R. Rohlfing, J. Doring, M. Pemk, *Angew. Chem.* **1991**, *103*, 575; *Angew. Chem. Int. Ed. Engl.* **1991**, *30*, 588; d) D. Hou, K. S. Hagen, C. L. Hill, *J. Am. Chem. Soc.* **1992**, *114*, 5864; e) D. Hou, K. S. Hagen, C. L. Hill, *J. Chem. Soc. Chem. Commun.* **1993**, 426; f) A. Muller, H. Reuter, S. Dillinger, *Angew. Chem.* **1995**, *107*, 2505; *Angew. Chem. Int. Ed. Engl.* **1995**, *34*, 2328; g) Y. Hayashi, K. Fukuyama, T. Takatera, A. Uehara, *Chem. Lett.* **2000**, 770.

[13] a) A. Muller, E. Krickemeyer, H. Bogge, M. Schmidtmann, F. Peters, C. Menke, J. Meyer, *Angew. Chem.* **1997**, *109*, 500; *Angew. Chem. Int. Ed. Engl.* **1997**, *36*, 484; b) A. Muller, S. Sarkar, S. Q. N. Shah, H. Bogge, M. Schmidtmann, P. Kogerler, B. Hauptfleisch, A. X. Trauwein, V. Schunemann, *Angew. Chem.* **1999**, *111*, 3435–3439; *Angew. Chem. Int. Ed.* **1999**, *38*, 3238–3241.

[14] a) R. C. Haushalter, L. A. Mundi, *Chem. Mater.* **1992**, *4*, 31; b) A. K. Cheetham, G. Férey, T. Loiseau, *Angew. Chem.* **1999**, *111*, 3466; *Angew. Chem. Int. Ed.* **1999**, *38*, 3268, and references therein; c) C. du Peloux, A. Dolbecq, P. Mialane, J. Marrot, E. Riviere, F. Secheresse, *Angew. Chem.* **2001**, *113*, 2521; *Angew. Chem. Int. Ed.* **2001**, *40*, 2455; d) C. du Peloux, P. Mialane, A. Dolbecq, J. Marrot, E. Riviere, F. Secheresse, *J. Mater. Chem.* **2001**, *11*, 3392.

[15] K. Y. Matsumoto, M. Kato, Y. Sasaki, *Bull. Acad. Vet. Fr. Bull. Chem. Soc. Japan* **1976**, *49*, 106.

[16] a) M. J. Manos, J. D. Woollins, A. M. Z. Slawin, T. A. Kabanos, *Angew. Chem.* **2002**, *114*, 2925–2929; *Angew. Chem. Int. Ed.* **2002**, *41*, 2801–2805; b) M. J. Manos, H. N. Miras, J. D. Woollins, V. Tangoulis, A. M. Z. Slawin, T. A. Kabanos, *Angew. Chem.* **2003**, *115*, 441–443; *Angew. Chem. Int. Ed.* **2003**, *42*, 425–427; c) D. Long, P. Kogerler, L. Cronin, *Angew. Chem.* **2004**, *116*, 1853–1856; *Angew. Chem. Int. Ed.* **2004**, *43*, 1817–1820.

[17] C. R. Brandt, V. Eldik, *Chem. Rev.* **1995**, *95*, 119.

[18] a) *Materials for Non-Linear Optics: Chemical Perspectives* (Eds.: G. D. Stucky, S. R. Marder, J. E. Sohn) American Chemical Society, Washington DC, **1991**; b) *Novel Optical Materials and Applications* (Eds.: I.C. Khoo, F. Simoni, C. Umeton), Wiley, New York, **1997**.

[19] a) W. T. A. Harrison, L. L. Dussack, A. J. Jacobson, *J. Solid State Chem.* **1996**, *125*, 234; b) P. S. Halasyamani, D. O'Hare, *Chem. Mater.* **1998**, *10*, 646, and references therein; c) W. T. A. Harrison, *Acta Crystallogr. Sect. C* **1999**, *55*, 1980; d) W. T. A. Harrison, M. L. F. Phillips, J. Stanchfield, T. M. Nenoff, *Angew. Chem.* **2000**, *112*, 3966; *Angew. Chem. Int. Ed.* **2000**, *39*, 3808; e) M. G. Johnston, W. T. A. Harrison, *Inorg. Chem.* **2001**, *40*, 6518.

[20] a) A. C. Bean, C. F. Campana, O. Kwon, T. E. Albrecht-Schmitt, *J. Am. Chem. Soc.* **2001**, *123*, 8806; b) A. C. Bean, S. M. Pepper, T. E. Albrecht-Schmitt, *Chem. Mater.* **2001**, *13*, 1266; c) R. E. Sykora, K. M. Ok, P. S. Halasyamani, T. E. Albrecht-Schmitt, *J. Am. Chem. Soc.* **2002**, *124*, 1951; d) R. E. Sykora, D. M. Wells, T. E. Albrecht-Schmitt, *Inorg. Chem.* **2002**, *41*, 2697.

[21] a) K. Inumaru, M. Misono, T. Okuhara, *Appl. Catal. A* **1997**, *149*, 133; b) P. J. Dunn, G. H. Stenger, E. I. Wachs, *Catal. Today* **1999**, *53*, 543; c) P. J. Dunn, G. H. Stenger, E. I. Wachs, *Catal. Today* **1999**, *51*, 301; d) O. B. Lapina, S. B. Balzhinimaev, S. Boghosian, K. M. Eriksen, R. Fehrmann, *Catal. Today* **1999**, *51*, 469.

[22] E. N. Baker, S. E. Palmer in *Porphyrins I* (Ed.: D. Dolphin) Academic Press, New York, **1978**.

[23] A. Muller, E. Krickenmeyer, M. Penk, H. J. Wallberg, H. Bogge, *Angew. Chem.* **1987**, *99*, 1060; *Angew. Chem. Int. Ed. Engl.* **1987**, *26*, 1045.

[24] Y. Hayashi, N. Miyakoshi, T. Shinguchi, A. Uehara, *Chem. Lett.* **2001**, 170.

[25] The trigonality index, τ, is given by the equation, $\tau = (\phi_1 - \phi_2)/60$, where ϕ_1, is the largest angle and ϕ_2 is next largest angle in the coordination sphere ($\tau = 0/1$ for square-pyramidal/trigonal-bipyramidal geometries, respectively); A. W. Anson, J. N. Rao, J. Reedijk, J. Rijn, G. C. Verschoor, *J. Chem. Soc. Dalton Trans.* **1984**, 1349.

[26] a) K. Dimitrou, K. Folting, W. E. Streib, G. Christou, *J. Chem. Soc. Chem. Commun.* **1994**, 1385; b) K. Dimitrou, A. D. Brown, K. Folting, W. E. Streib, G. Christou, *Inorg. Chem.* **1999**, *38*, 1834.

[27] B. Gail Karet, Z. Sun, E. W. Streib, J. C. Bollinger, D. N. Hendrickson, G. Christou, *Chem. Commun.* **1999**, 2249.

[28] a) L. Hailian, C. E. Davis, T. L. Groy, D. G. Kelley, O. M. Yaghi, *J. Am. Chem. Soc.* **1998**, *120*, 2186; b) R. I. Walton, F. Millange, T. Loiseau, D. O'Hare, G. Férey, *Angew. Chem.* **2000**, *112*, 4726–4729; *Angew. Chem. Int. Ed.* **2000**, *39*, 4552–4555.

[29] P. K. Nakamoto, *Infrared and Raman Spectra of Inorganic and Coordination Compounds*, Wiley, New York, **1986**.

[30] a) A. Barra, D. Gatteschi, L. Pardi, A. Miiller, J. Doring, *J. Am. Chem. Soc.* **1992**, *114*, 8509–8514; b) D. Gatteschi, B. Tsukerblatt, A. L. Barra, L. C. Brunel , A. Miller, J. Wring, *Inorg. Chem.* **1993**, *32*, 2114; c) G. B. Karet, Z. Sun, D. D. Heinrich, J. K. McCusker, K. Folting, W. E. Streib, J. C. Huffman, D. N. Hendrickson, G. Christou, *Inorg. Chem.* **1996**, *35*, 6450.

[31] J. C. Bonner, M. E. Fisher, *Phys. Rev. A* **1964**, *135*, 640.

[32] W. E. Estes, D. P. Gavel, W. E. Hatfield, D. Hodgson, *Inorg. Chem.* **1978**, *17*, 1415.

[33] L. Deakin, A. M. Arif, J. S. Miller, *Inorg. Chem.* **1999**, *38*, 5072.

[34] P. J. Hay, J. C. Thibeault, R. Hoffmann, *J. Am. Chem. Soc.* **1975**, *97*, 4884.

[35] *SMART-NT Software Reference Manual*, version 5.059, Bruker AXS, Inc., Madison, WI, **1998**.

[36] *SAINT+ Software Reference Manual*, version 6.02, Bruker AXS, Inc., Madison, WI, **1999**.

[37] G. M. Sheldrick, SHELXS-90, Program for the Solution of Crystal Structure, University of Göttingen (Germany), **1986**.

[38] G. M. Sheldrick, SHELXL-97, Program for the Refinement of Crystal Structure, University of Göttingen (Germany), **1997**.

[39] *SHELXTL-NT Software Reference Manual*, version 5.1, Bruker AXS, Inc., Madison, WI, **1998**.

[40] A. D. Becke, *J. Chem. Phys.* **1993**, *98*, 5648.

[41] C. Lee, W. Yang, Parr, R. G. *Phys. Rev. B* **1988**, *37*, 785.

[42] P. J. Hay, W. R. Wadt, *J. Chem. Phys.* **1985**, *82*, 299.

[43] T. H. Dunning, Jr., P. J. Hay, in *Modern Theoretical Chemistry*, *Vol. 3* (Ed.: H. F. Schaefer, III), Plenum, New York, **1976**, 1.

[44] M. J. Frisch, G. W. Trucks, H. B. Schlegel, G. E. Scuseria, M. A. Robb, R. Cheeseman, V. G. Zakrzewski, J. A. Montgomery, Jr., R. E. Stratman, J. C. Burant, S. Dapprich, J. M. Millam, A. D. Daniels, K. N. Kudin, M. C. Strain, O. Farkas, J. Tomasi, V. Barone, M. Cossi, R. Cammi, B. Mennucci, C. Pomelli, C. Adamo, S. Clifford, J. Ochterski, G. A. Petersson, P. Y. Ayala, Q. Cui, K. Morokuma, P. Salvador, J. J. Dannenberg, D. K. Malick, A. D. Rabuck, K. Raghavachari, J. B. Foresman, J. Cioslowski, J. V. Ortiz, A. G. Baboul, B. B. Stefanov, G. Liu, A. Liashenko, P. Piskorz, Komaromi,I. R. Gomperts, R. L. Martin, D. J. Fox, T. Keith, M. A. Al-Laham, C. Y. Peng, A. Nanayakkara, M. Challacombe, P. M. W. Gill, B. Johnson, W. Chen, M. W. Wong, J. L. Andres, C. Gonzalez, M. Head-Gordon, E. S. Replogle, J. A. Pople, Gaussian 98, Revision A.7, Gaussian Inc., Pittsburgh PA, **1998**.

[45] M. E. Baldwin, *J . Chem. Soc.* **1961**, 3123.

[46] G. Newman, D. B. Pwell, *Spectrochim. Acta* **1963**, *19*, 213.

Received: March 2, 2004
Revised: November 23, 2004
Published online: February 1, 2005